scientific report

NLRX1 is a mitochondrial NOD-like receptor that amplifies NF-κB and JNK pathways by inducing reactive oxygen species production

Ivan Tattoli[1], Leticia A. Carneiro[1], Muguette Jéhanno[2], Joao G. Magalhaes[3], Youmin Shu[4], Dana J. Philpott[3], Damien Arnoult[5] & Stephen E. Girardin[1+]

[1]Department of Laboratory Medicine and Pathobiology, Medical Sciences Building, University of Toronto, Toronto, Ontario, Canada, [2]Groupe Polarité et Migration Cellulaires, Institut Pasteur, Paris, France, [3]Department of Immunology, Medical Sciences Building, University of Toronto, Toronto, Ontario, Canada, [4]Origene Technologies, Rockville, Maryland, USA, and [5]Inserm U542, Hopital Paul Brousse, Villejuif, France

NOD-like receptors (NLRs) are a family of intracellular sensors of microbial- or danger-associated molecular patterns. Here, we report the identification of NLRX1, which is a new member of the NLR family that localizes to the mitochondria. NLRX1 alone failed to trigger most of the common signalling pathways, including nuclear factor-κB (NF)-κB- and type I interferon-dependent cascades, but could potently trigger the generation of reactive oxygen species (ROS). Importantly, NLRX1 synergistically potentiated ROS production induced by tumour necrosis factor α, *Shigella* infection and double-stranded RNA, resulting in amplified NF-κB-dependent and JUN amino-terminal kinases-dependent signalling. Together, these results identify NLRX1 as a NLR that contributes to the link between ROS generation at the mitochondria and innate immune responses.
Keywords: NLRX1; NOD-like receptors; mitochondria; reactive oxygen species; NF-κB; innate immunity

INTRODUCTION

The innate immune system relies on the detection of microbial-associated molecular patterns (MAMPs) or danger-associated molecular patterns (DAMPs) by using host pattern recognition

[1]Department of Laboratory Medicine and Pathobiology, Medical Sciences Building, University of Toronto, Toronto, Ontario, Canada M5S 1A8
[2]Groupe Polarité et Migration Cellulaires, Institut Pasteur, 25 Rue du Dr Roux, Paris cedex 15 75724, France
[3]Department of Immunology, Medical Sciences Building, University of Toronto, Toronto, Ontario, Canada M5S 1A8
[4]Origene Technologies, 6 Taft Court, Rockville, Maryland 20850, USA
[5]Inserm U542, Hopital Paul Brousse, Villejuif, France
[+]Corresponding author. Tel: +1 416 978 75 07; Fax: +1 416 978 59 59;
E-mail: stephen.girardin@utoronto.ca

molecules (PRMs). TOLL-like receptors (TLRs) represent a class of membrane-spanning PRMs that have been studied extensively in the past decade (Akira & Takeda, 2004). More recently, NOD-like receptors (NLRs) have emerged as a second family of PRMs that are expressed intracellularly and detect various MAMPs and DAMPs (Fritz *et al*, 2006; Meylan *et al*, 2006). A subgroup of NLRs, represented by NOD1 and NOD2, triggers pro-inflammatory cascades, such as nuclear factor-κB (NF)-κB, p38 and JUN amino-terminal kinases (JNK) MAP kinases, in response to bacterial peptidoglycan and bacterial infections. The other NLRs characterized so far (including NALP1–3, IPAF and NAIP) are implicated in the induction of the caspase 1 inflammasome, in response to various MAMPs and DAMPs (Fritz *et al*, 2006; Meylan *et al*, 2006).

RESULTS AND DISCUSSION

It is known that mitochondria have a role in the innate immunity against microbial pathogens by promoting apoptotic pathways. In addition, emerging evidence indicates that microbial-induced necrosis is related to changes in mitochondrial membrane potential, but it remains unclear whether these events are a consequence of a global mitochondrial metabolism collapse or early signals to promote necrotic cell death (Golstein & Kroemer, 2007). Furthermore, mitochondria have recently gained recognition in contributing to viral immunity, with the identification of IPS1/MAVS/VISA/Cardif, which is a crucial protein that acts as an adapter for RIG-I and MDA5 viral RNA sensors localized in the mitochondria (Fritz *et al*, 2006; Meylan *et al*, 2006). Finally, mitochondria represent one of the main centres of production of reactive oxygen species (ROS) within the cell. ROS are directly microbiocidal and, in addition, are important for amplifying pro-inflammatory pathways, such as NF-κB and JNK (Gloire *et al*, 2006). Importantly, although there is a considerable literature showing the direct role of ROS in antimicrobial defence, the

signalling pathways linking microbial detection and ROS production remain poorly defined. Here, we report the identification of NLRX1, the first member of the NLR family to localize to a specific organelle. Accordingly, we show that the N-terminal region of NLRX1 targets the molecule to the mitochondria. Strikingly, our results identify NLRX1 as an activator for the generation of ROS, and show that the protein amplifies NF-κB- and JNK-dependent signalling. NLRX1 is the first reported NLR that specifically controls ROS production.

The human genome database shows the existence of *NLRX1*, an uncharacterized NLR on the 11q23.3 locus that gives rise to a protein of 975 amino acids (accession no NP_078894). NLRX1 shows a typical NACHT (present in NAIP, CIITA, HET-E and TP1) domain between amino acids 160 and 325, and a carboxy-terminal LRR domain comprised of seven repeats, from amino acids 679 to 975 (Fig 1A). The N-terminal region of NLRX1, however, has no homology to any known domain, but shows strong conservation between several mammalian NLRX1 orthologues (Fig 1B) and is predicted by algorithms (such as SMART) to contain a mitochondrial N-terminal targeting pre-sequence in the first 40 amino acids. Interestingly, *in silico* phylogenetic analysis of LRR domains from human NLRs shows that NLRX1 LRR has homology with a subgroup of NLRs composed of NOD1, NOD2, NOD3, NOD27 and CIITA (Fig 1C). Finally, NLRX1 was found to be expressed ubiquitously in human tissues, with the strongest expression observed in mammary gland, heart and muscle (Fig 1D), and was constitutively expressed in several human cell lines (supplementary Fig 1 online).

We generated deletion constructs of NLRX1 that were tagged on the C terminus with a Flag epitope (Fig 2A). These constructs, which were overexpressed in human embryonic kidney 293T (HEK293T) cells, were detected by immunoblotting as single bands at the expected molecular weight (Fig 2B). Next, NLRX1 was overexpressed in HeLa cells and the subcellular localization of the protein was determined by using immuno-fluorescence. NLRX1 localized exclusively into filamentous structures, indicating that the protein was associated with cellular organelles (Fig 2C). Interestingly, the NLRX1 N-ter, but not the NLRX1 ΔN-ter construct, was found to also localize into these subcellular structures, implying that the first 156 amino acids of NLRX1 must contain an organelle-specific addressing sequence (Fig 2C). By using a dye that specifically stains mitochondria (MitoTracker), we showed by confocal microscopy that NLRX1 colocalizes with mitochondria (Fig 2D). By using a biochemical approach, we carried out stepwise fractionation of NLRX1-overexpressing HEK293T cells and found that NLRX1 was present in cellular membrane fractions (Fig 2E)—in heavy- but not light-membrane fractions (Fig 2F)—and in an isolated mitochondrial fraction (Fig 2G). Finally, we generated a polyclonal antibody against a peptide from NLRX1 and observed that the endogenous NLRX1 colocalized with mitochondria in HeLa and MCF-7 (human breast adeno-carcinoma) cells (Fig 2H).

Next, we investigated whether NLRX1 could activate some of the well-described signal transduction pathways. HEK293T cells were transfected with NLRX1 along with reporter-driven luciferase constructs. NLRX1 failed to stimulate NF-κB-, interferon-stimulated response element (ISRE)-, AP1-, p53- and hypoxia-inducible factor (HIF)-dependent reporter genes (Fig 3A,B; supplementary

Fig 2 online). In addition, we failed to identify a significant role for NLRX1 in the modulation of the extrinsic or intrinsic modes of apoptosis, using staurosporine and tumour necrosis factor α (TNFα) plus cycloheximide (CHX) as inducers of apoptosis (supplementary Fig 3 online). By contrast, NLRX1 overexpression could trigger the production of ROS to levels similar to those induced by TNFα, a well-characterized activator of ROS (Fig 3C). We also observed that targeting of NLRX1 to the mitochondria was required for ROS activation, as NLRX1 ΔN-ter overexpression was unable to stimulate ROS production (Fig 3D). Importantly, we showed that NLRX1-mediated ROS production was not an artefact of overexpressing the protein to the mitochondria, as NLRX1 N-ter overexpression failed to induce ROS production (Fig 3D).

Several pro-inflammatory stimuli are known to trigger ROS generation, such as TNFα stimulation, bacterial and viral infections (Gloire *et al*, 2006), and we aimed to determine whether NLRX1 could potentiate these responses. Indeed, HeLa cells transfected with NLRX1 significantly increased ROS production induced by TNFα, *Shigella* infection and poly-inosinic:polycytidylic acid (poly I:C), a synthetic molecule that mimics double-stranded RNA from viruses (Fig 4A). These results indicate that NLRX1 overexpression upregulates ROS production triggered by several stimuli. Time-course experiments showed that the potentiation effect of NLRX1 on ROS production could be observed in early time points (15 min for TNFα stimulation and 45 min for *Shigella* infection; Fig 4B), and at later time points (supplementary Fig 4 online). As it is well established that ROS production potentiates pro-inflammatory pathways triggered by various stimuli, such as NF-κB and JNK (Gloire *et al*, 2006), we analysed the effect of NLRX1 overexpression on NF-κB and JNK pathways induced by TNFα and *Shigella*; poly I:C was not added to these experiments as it seemed to be a poor activator of NF-κB and JNK in our experimental system. By using immunofluore-scence, we measured NF-κB p65 subunit translocation over time in cells transfected with NLRX1 or not, following either stimulation with TNFα or infection with *Shigella* (see supplementary Fig 5 online for details). In the case of *Shigella* infection, we observed that NLRX1-positive cells showed increased p65 translocation as early as 15 min after infection, an effect that was maintained over time (Fig 4C). As NLRX1-dependent upregulation of ROS following *Shigella* infection could be observed only 45 min after infection (see above), it is likely that the positive effect of NLRX1 on *Shigella*-induced NF-κB activation between 15 min and 45 min might result from ROS-independent effects. By contrast, in the case of TNFα stimulation, the difference between NLRX1 over-expressing cells and non-transfected cells could only be observed at later time points (Fig 4D). Similar experiments were carried out using NLRX1 ΔN-ter and, as for ROS generation (see above Fig 3C), this construct was unable to potentiate NF-κB pathway triggered by TNFα stimulation or *Shigella* infection (supplementary Fig 6 online). Next, we analysed the impact of NLRX1 on the degradation of IκBα, a crucial inhibitory molecule of the NF-κB pathway. We observed that NLRX1 overexpression resulted in increased and prolonged degradation of IκBα in response to *Shigella* infection (Fig 4E) and TNFα (Fig 4F). Similarly, we also observed that NLRX1 potentiated JNK activation triggered by these two stimuli, as observed by immunoblotting with an antibody specific for the phosphorylated form of JNK. Again, we observed
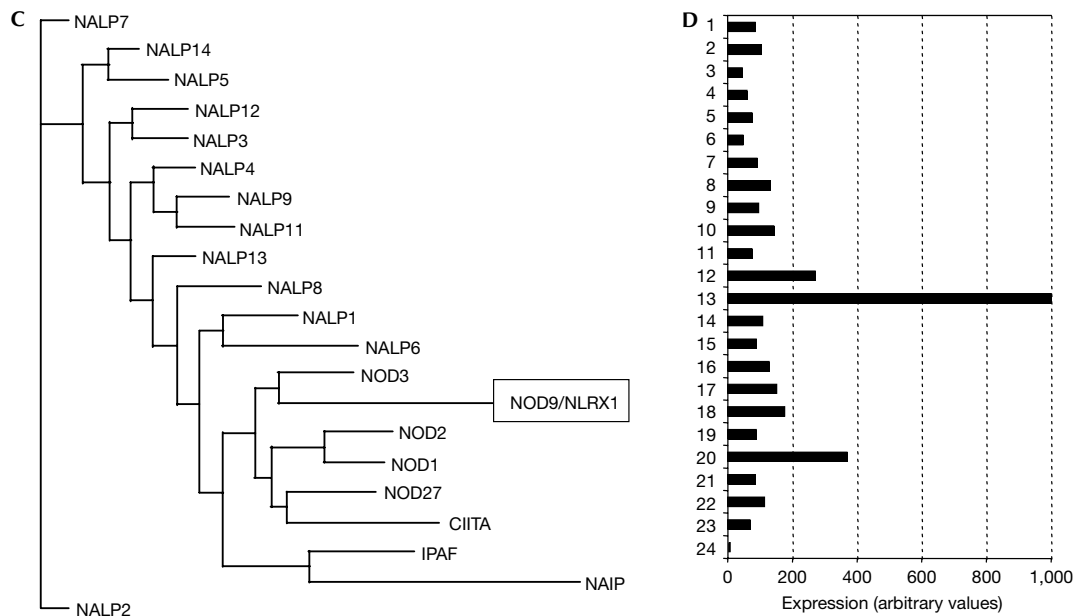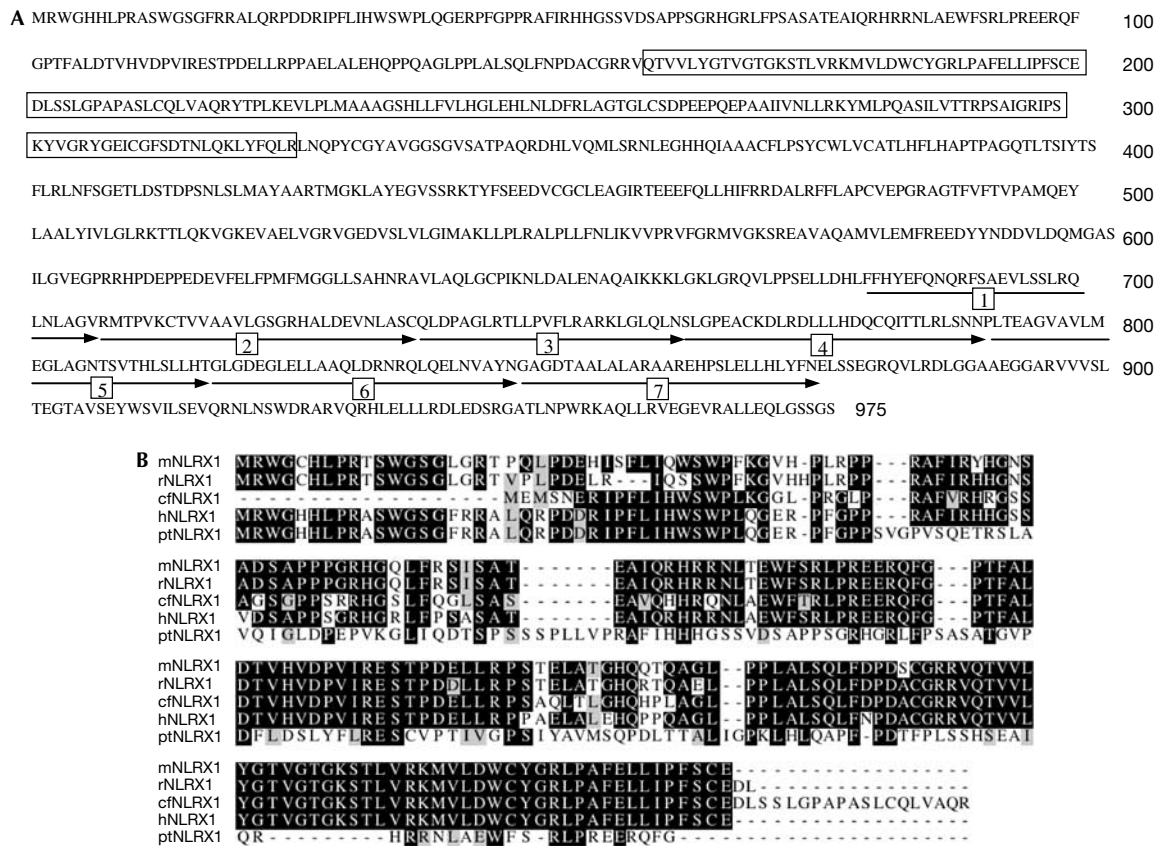
A

```
MRWGHHLPRASWGSGFRRALQRPDDRIPFLIHWSWPLQGERPFGPPRAFIRHHGSSVDSAPPSGRHGRLFPSASATEAIQRHRRNLAEWFSRLPREERQF   100
GPTFALDTVHVDPVIRESTPDELLRPPAELALEHQPPQAGLPPLALSQLFNPDACGRRV QTVVLYGTVGTGKSTLVRKMVLDWCYGRLPAFELLIPFSCE   200
DLSSLGPAPASLCQLVAQRYTPLKEVLPLMAAAGSHLLFVLHGLEHLNLDFRLAGTGLCSDPEEPQEPAAIIVNLLRKYMLPQASILVTTRPSAIGRIPS   300
KYVGRYGEICGFSDTNLQKLYFQLR LNQPYCGYAVGGSGVSATPAQRDHLVQMLSRNLEGHHQIAAACFLPSYCWLVCATLHFLHAPTPAGQTLTSIYTS   400
FLRLNFSGETLDSTDPSNLSLMAYAARTMGKLAYEGVSSRKTYFSEEDVCGCLEAGIRTEEEFQLLHIFRRDALRFFLAPCVEPGRAGTFVFTVPAMQEY   500
LAALYIVLGLRKTTLQKVGKEVAELVGRVGEDVSLVLGIMAKLLPLRALPLLFNLIKVVPRVFGRMVGKSREAVAQAMVLEMFREEDYYNDDVLDQMGAS   600
ILGVEGPRRHPDEPPEDEVFELFPMFMGGLLSAHNRAVLAQLGCPIKNLDALENAQAIKKKLGKLGRQVLPPSELLDHLFFHYEFQNQRFSAEVLSSLRQ   700
LNLAGVRMTPVKCTVVAAVLGSGRHALDEVNLASCQLDPAGLRTLLPVFLRARKLGLQLNSLGPEACKDLRDLLLHDQCQITTLRLSNNPLTEAGVAVLM   800
EGLAGNTSVTHLSLLHTGLGDEGLELLAAQLDRNRQLQELNVAYNGAGDTAALALARAAREHPSLELLHLYFNELSSEGRQVLRDLGGAAEGGARVVVSL   900
TEGTAVSEYWSVILSEVQRNLNSWDRARVQRHLELLLRDLEDSRGATLNPWRKAQLLRVEGEVRALLEQLGSSGS   975
```

B

```
          ┌─────────────────────────────────────────────────────┐
mNLRX1   MRWGCHLPRTSWGSGLGRT PQLPDEHISFLIQWSWPFKGVH-PLRPP---RAFIRYHGNS
rNLRX1   MRWGCHLPRTSWGSGLGRTVPLPDELR---IQSSWPFKGVHHPLRPP---RAFIRHHGNS
cfNLRX1         MEMSNERIPFLIHWSWPLKGGL-PRGLP---RAFVRHRGSS
hNLRX1   MRWGHHLPRASWGSGFRRALQRPDDRIPFLIHWSWPLQGER-PFGPP---RAFIRHHGSS
ptNLRX1  MRWGHHLPRASWGSGFRRALQRPDDRIPFLIHWSWPLQGER-PFGPPSVGPVSQETRSLA

mNLRX1   ADSAPPPGRHGQLFRSISAT------EAIQRHRRNLTEWFSRLPREERQFG---PTFAL
rNLRX1   ADSAPPPGRHGQLFRSISAT------EAIQRHRRNLTEWFSRLPREERQFG---PTFAL
cfNLRX1  AGSGPPSRRHGSLFQGLSAS------EAVQHRQNLAEWFIRLPREERQFG---PTFAL
hNLRX1   VDSAPPSGRHGRLFPSASAT------EAIQRHRRNLAEWFSRLPREERQFG---PTFAL
ptNLRX1  VQIGLDPEPVKGLIQDTSPSSSPLLVPRAFIHHHGSSVDSAPPSGRHGRLFPSASATGVP

mNLRX1   DTVHVDPVIRESTPDELLRPSTELATGHQQTQAGL--PPLALSQLFDPDSCGRRVQTVVL
rNLRX1   DTVHVDPVIRESTPDDLLRPSTELATGHQRTQAEL--PPLALSQLFDPDACGRRVQTVVL
cfNLRX1  DTVHVDPVIRESTPDELLRPSAQLTLGHQHPLAGL--PPLALSQLFDPDACGRRVQTVVL
hNLRX1   DTVHVDPVIRESTPDELLRPPAELALEHQPPQAGL--PPLALSQLFNPDACGRRVQTVVL
ptNLRX1  DFLDSLYFLRESCVPTIVGPSIYAVMSQPDLTTALIGPKLHLQAPF-PDTFPLSSHSEAI

mNLRX1   YGTVGTGKSTLVRKMVLDWCYGRLPAFELLIPFSCE----------
rNLRX1   YGTVGTGKSTLVRKMVLDWCYGRLPAFELLIPFSCEDL--------
cfNLRX1  YGTVGTGKSTLVRKMVLDWCYGRLPAFELLIPFSCEDLSSLGPAPASLCQLVAQR
hNLRX1   YGTVGTGKSTLVRKMVLDWCYGRLPAFELLIPFSCE----------
ptNLRX1  QR------HRRNLAEWFS-RLPREERQFG
```

C

D

Fig 1 | Characterization of NLRX1. (**A**) Amino-acid sequence of NLRX1. The NACHT domain is indicated by boxes, and the seven repeats of the LRR domain are numbered and indicated by arrows. (**B**) Sequence alignment of NLRX1 amino-terminal region from mouse (mNLRX1), rat (rNLRX1), *Canis familiaris* (cfNLRX1), human (hNLRX1) and *Pan troglodytes* (ptNLRX1). The residues identical and similar to those of NLRX1 are shown by reverse and dark highlighting, respectively. (**C**) The phylogenetic tree of NLR LRR domains was created using ClustalW and Neighbour-Joining/UPGMA method version 3.6a3 algorithms. (**D**) Expression profile of NLRX1 in a panel of 24 human tissues: (1) uterus; (2) thyroid; (3) thymus; (4) testis; (5) stomach; (6) spleen; (7) skin; (8) prostate; (9) pituitary; (10) pancreas; (11) ovary; (12) muscle; (13) mammary gland; (14), lymphocytes; (15) lymph nodes; (16) lung; (17) liver; (18) kidney; (19) intestine; (20) heart; (21) colon; (22) brain; (23) bone marrow; and (24) adrenal gland. NLR, NOD-like receptor.
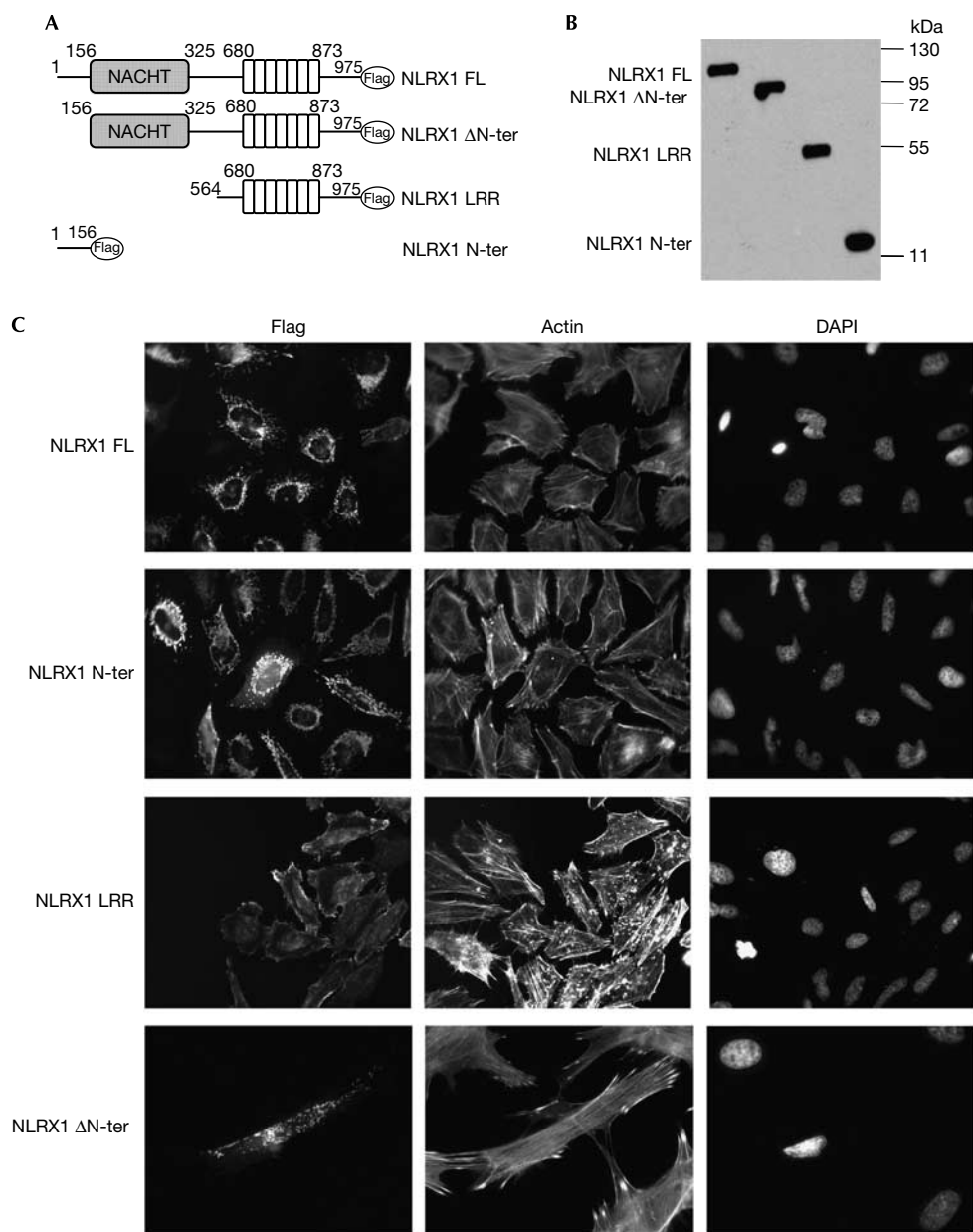
Fig 2 | NLRX1 is a mitochondria-associated protein. (**A**) Schematic representation of the NLRX1 constructs. (**B**) Expression profile of NLRX1 constructs determined by western blotting using a Flag antibody. (**C**) Immunofluorescence analysis of Flag-tagged NLRX1 constructs expressed in HeLa cells using a Flag antibody. Filamentous actin and nuclei were stained using rhodamin-conjugated phalloidin and DAPI, respectively. (**D**) Confocal microscopy analysis of NLRX1-overexpressing HeLa cells, stained for NLRX1 (Flag antibody) and mitochondria (MitoTracker dye). (**E–G**) Cellular fractions of NLRX1-Flag-transfected HEK293 cells were obtained by using specific lysis buffers and analysed by western blotting using antibodies against PARP (nuclear protein), Calnexin (endoplasmic reticulum protein), Hsp60 (mitochondrial protein) and caspase 3 (cytosolic protein). Stepwise fractionation shows that NLRX1 is present in (**E**) membrane, (**F**) heavy membrane and (**G**) mitochondrial fractions. (**H**) Mitochondrial localization of endogenous NLRX1 in MCF-7 and HeLa cells, using a rabbit polyclonal NLRX1 antibody and detection of mitochondria with MitoTracker. CF, cytosolic fraction; DAPI, 4,6-diamidino-2-phenylindole; HEK293, human embryonic kidney 293 cells; HM, heavy membrane fraction; HSP, heat shock protein; IM, isolated mitochondria; LM, light membrane fraction; MF; membrane fraction; NF, nuclear fraction; NLR, NOD-like receptor; PARP, poly (ADP-ribose) polymerase.

that NLRX1 increased JNK activation early in the *Shigella* infection (15′–30′; Fig 4G), whereas enhancing TNFα-mediated JNK activation later (Fig 4H).

NLRX1 is the first reported NLR that specifically associates with a cellular organelle, the mitochondria. The protein was found to be expressed ubiquitously, with a higher expression observed
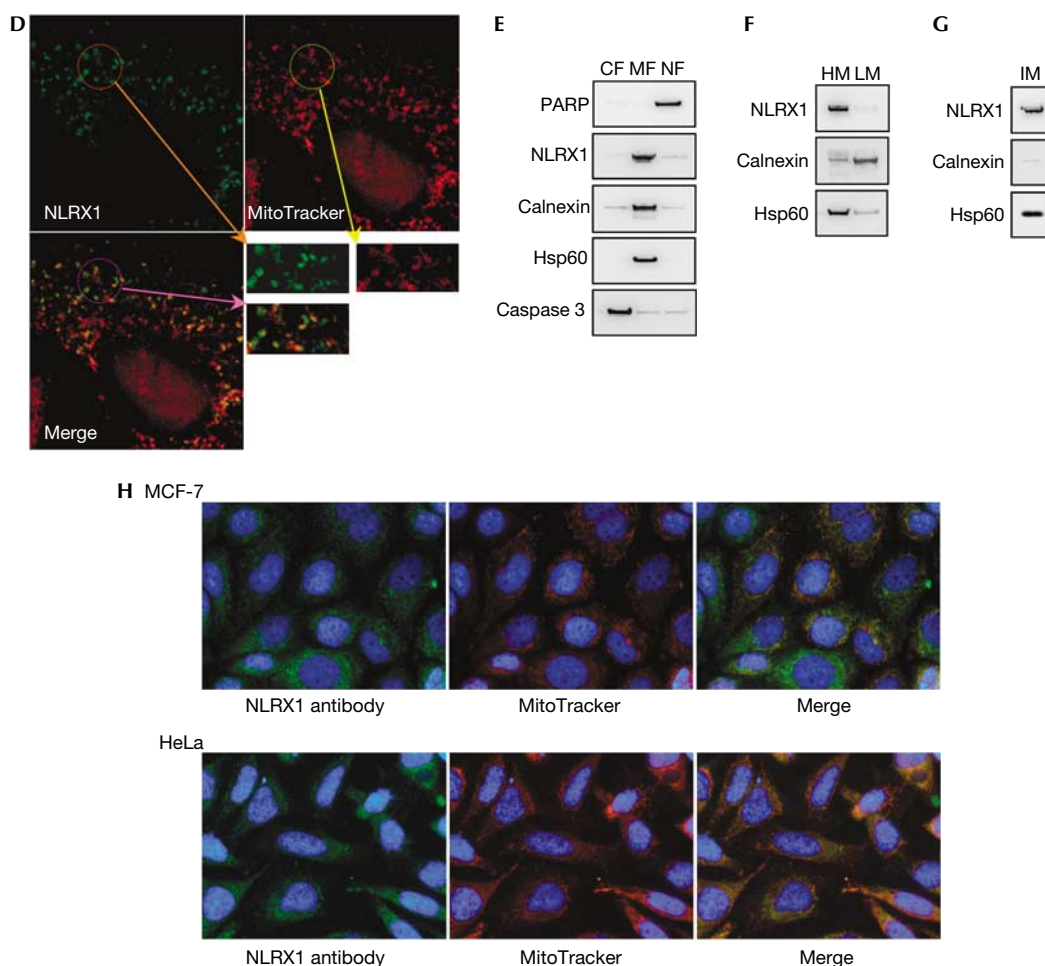
Fig 2 | Continued.

in tissues containing muscular cells (heart, skeletal muscle and mammary gland), which might reflect the accumulation of this organelle in tissues with high metabolic requirements. We also observed that NLRX1 specifically triggered the generation of ROS, which is consistent with the subcellular localization profile of NLRX1. The ability of this NLR family member to trigger ROS generation is likely to be of importance for the development of the innate immune response. Indeed, several cell-signalling events, especially in the NF-κB pathway, require ROS production as general ROS inhibitors have been shown by many groups over the years to inhibit activation (Gloire *et al*, 2006). Triggering of molecules like NLRX1, therefore, might be required for ROS generation and thereby contribute to innate immune signalling. In accordance with this, our findings, which follow the kinetics of ROS production following infection (in minutes), indicate that ROS are not generated as a side effect of the induction of other pathways, but are *per se* the targets of specific cell signalling. These data are the first to indicate, therefore, that specific cell activation of an innate immune receptor regulates specifically the generation of ROS.

Probably the most important question that arises from our study relates to the nature of the endogenous stimulus sensed by NLRX1, which then triggers NRLX1-dependent ROS production by the

mitochondria. Indeed, it is reasonable to speculate that NLRX1, similar to the other members of the NLR family characterized so far, specifically senses a microbial- or a danger-signal-derived molecular signature. Bacterial pathogens and viruses are good candidates for natural NLRX1 activators as many of those are known to induce ROS production following infection. Further research will address which specific MAMP or DAMP is required for NLRX1 activation.

We have shown that the mitochondrial targeting of NLRX1 is crucial for triggering ROS and, conversely, that the over-expression of the N-terminal domain of NLRX1, although being targeted to the mitochondria, is not sufficient to induce ROS. This indicates that the interaction of NLRX1 with mitochondrial proteins through the NACHT or LRR domains might be crucial for the generation of ROS. Future studies should show the nature of NLRX1-interacting proteins in the mitochondria that regulate ROS generation.

Mitochondria are emerging as an organelle of crucial importance for the regulation of innate immune responses. The mitochondrial localization of IPS1/MAVS/VISA/Cardif is likely associated with its ability to trigger NF-κB and type I interferon responses (Seth *et al*, 2005). It has been reported that ASC/TMS1, a crucial adaptor molecule of the caspase 1 inflammasome is also
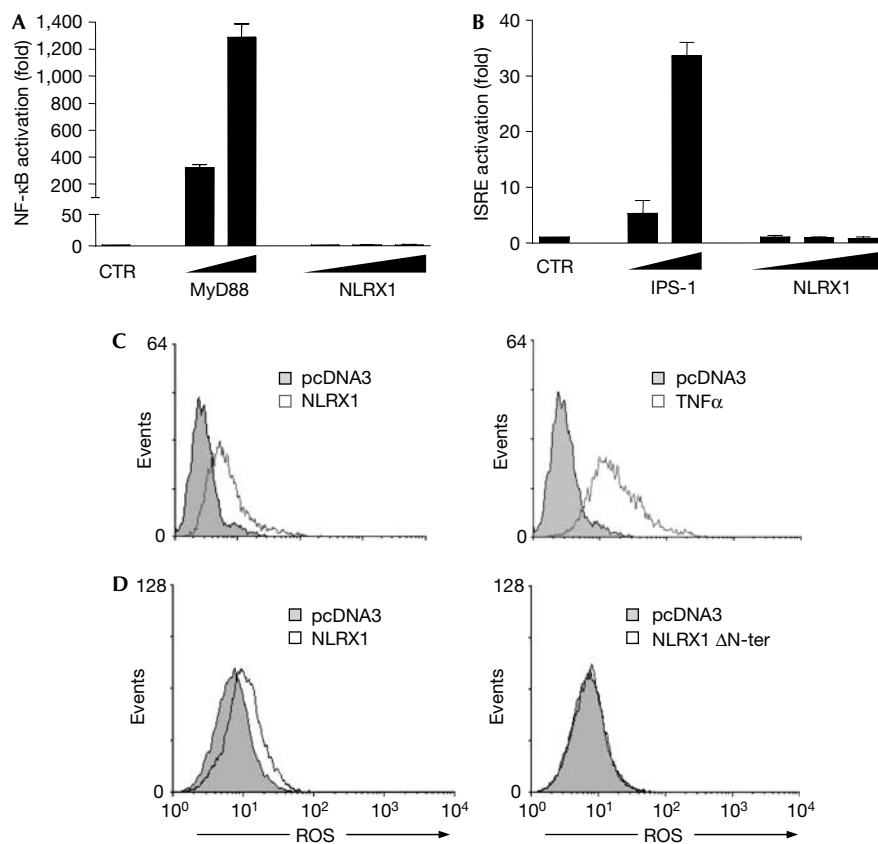
Fig 3 | NLRX1 triggers the generation of ROS. (**A,B**) HEK293T epithelial cells were transfected with increasing amounts (10, 100 and 250 ng) of NLRX1 expression vector together with luciferase-reporter constructs of (**A**) NF-κB and (**B**) interferon-stimulated response element (ISRE). Overexpression of MyD88 (**A**) or IPS-1 (**B**) were used as positive controls. Data shown are the mean ± s.e.m. of duplicates and are representative of three independent experiments. (**C**) HeLa cells were transfected overnight with pcDNA3 or NLRX1 vectors (left), or with pcDNA3 followed by stimulation for 1 h with 10 ng/ml TNFα (right). ROS production was measured by using a redox-sensitive dye (CM-H₂DCFDA) on live cells, followed by flow cytometry analysis. (**D**) HeLa cells were transfected overnight with pcDNA3, NLRX1, NLRX1 ΔN-ter or NLRX1 N-ter vectors and ROS were measured as in (**C**). CTR, control; HEK293, human embryonic kidney 293 cells; NF-κB, nuclear factor-κB; NLR, NOD-like receptor; ROS, reactive oxygen species; TNFα, tumour necrosis factor α.

partly associated with mitochondria (Ohtsuka *et al*, 2004). Whether this specific role of mitochondria is related to its similarities with an ancestral bacterium, or is associated with the unique biophysical properties of the mitochondrial membranes, still remains to be determined.

METHODS

Reagents and cell culture. Actin-phalloidin (R-415, Invitrogen, Carlsbad, CA, USA; dilution 1:100) and 4,6-diamidino-2-phenyl-indole (DAPI; Sigma, St Louis, MO, USA; 1:1000) were added to fixed cells. Phorbol 12-myristate 13-acetate (Sigma) was added to cells for 4 h (1:1,000). MitoTracker Red CMXRos (1:8,000; Invitrogen) was added to live cells according to manufacturer's specifications. Recombinant human TNFα (210-TA/CF; 10 ng/ml) was obtained from R&D Systems (Minneapolis, MN, USA). Poly I:C (10 μg/ml), staurosporine and CHX were from Sigma.

HEK293T and HeLa cells (American Type Culture Collection) were cultured in DMEM with HEPES 10 mM, supplemented with glutamine 2 mM and 5% Fetal Calf Serum (FCS; Invitrogen, Toronto, ON, Canada).

Antibodies. Mouse monoclonal anti-Flag M2 (Sigma; 1:1,000), anti-poly (ADP-ribose) polymerase (PARP; clone C2-10; BD Biosciences, Le Pont de Claire, France; 1:2,000), anti-calnexin (clone 37; BD Biosciences; 1:1,000), anti-Hsp60 (clone 24; BD Biosciences; 1:2,000) and mouse monoclonal anti-Tubulin (Sigma; 1:10,000) were used. Rabbit polyclonal anti-caspase 3 (Cell Signaling, Danvers, MA, USA; 1:1,000), anti-IκBα (sc-371; Santa Cruz Biotechnology, Santa Cruz, CA, USA; 1:500), anti-phospho-JNK (Cell Signaling; 1:700), anti-NF-κB p65 (sc-371, Santa Cruz Biotechnology; 1:500) and anticleaved caspase 3 and caspase 8 (Cell Signaling; 1:2,000) were used. Rabbit and mouse horseradish peroxydase-coupled antibodies were from Pierce Biotechnology (Rockford, IL, USA; 1:10,000). DyLight547-coupled rabbit and mouse antibodies were from Pierce Biotechnology (1:800 and 1:200, respectively). The NLRX1 polyclonal antibody was raised against a peptide in the region between
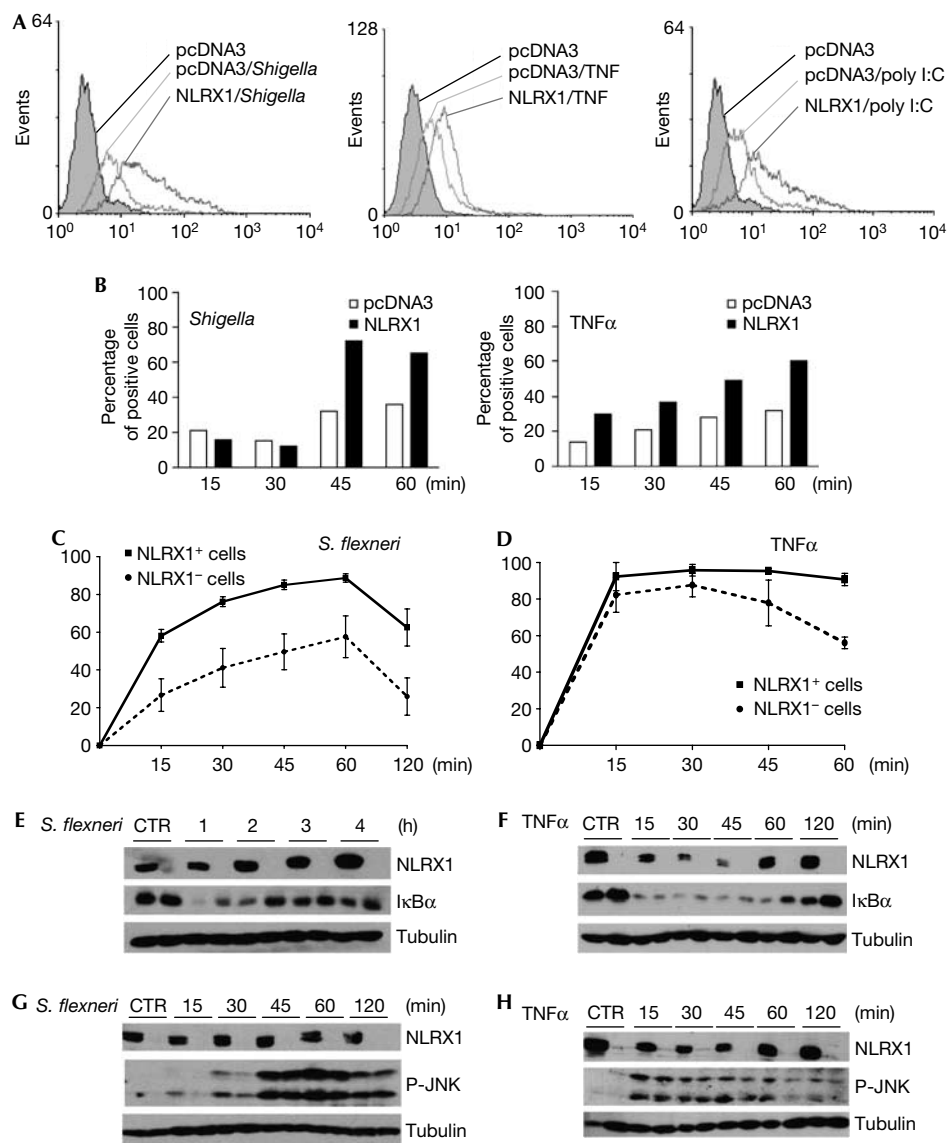
Fig 4 | Effect of NLRX1 on signalling pathways triggered by TNFα and *Shigella*. (**A**) HeLa cells were transfected overnight with pcDNA3 or NLRX1 vectors and infected for 1 h with *Shigella* (left), or stimulated for 1 h with 10 ng/ml TNFα (middle) or 3 h with 10 µg/ml poly I:C (right). ROS production was measured by using a redox-sensitive dye (CM-H₂DCFDA) on live cells, followed by flow cytometry analysis. (**B**) Time-course analysis of ROS production induced by *Shigella* (left) and TNFα (right) in conditions as in (**A**). (**C,D**) HeLa cells grown on glass coverslips were transfected overnight with NLRX1 expression vector and infected with (**C**) *Shigella* or (**D**) stimulated with 10 ng/ml TNFα for various times, as indicated. The nuclear translocation of NF-κB p65 subunit (as an indicator of the activation of the NF-κB pathway) was evaluated by immunofluorescence in cells overexpressing NLRX1 (NLRX1⁺) or not (NLRX1⁻). Data shown are the mean ± s.e.m. of three independent experiments, and for each condition and time point a minimum of 500 cells were counted. (**E–H**) HEK293T cells were transfected overnight with NLRX1 expression vector or pcDNA3 and infected with (**E,G**) *Shigella flexineri* or (**F,H**) stimulated with 10 ng/ml TNFα for different time periods, as indicated, and extracts were immunoblotted with antibodies against (**E,F**) IκBα or (**G,H**) phospho-JNK. NLRX1 expression was assessed using an Flag antibody and tubulin was used as a control for protein levels. CM-H₂DCFDA, 5-(and-6)-chloromethyl-2′,7′-dichlorodihydro-fluorescein diacetate, acetyl ester; CTR, control; HEK293, human embryonic kidney 293 cells; NF-κB, nuclear factor-κB; NLR, NOD-like receptor; poly I:C, polyinosinic:polycytidylic acid; ROS, reactive oxygen species; TNFα, tumour necrosis factor α.

the NACHT and LRR domains (Cederlane Labs, Burlington, ON, Canada).

NLRX1 expression constructs. Full-length NLRX1 (isoform 1; 975 amino acids; fully sequenced), cloned into pCMV6-XL6 expression vector was obtained from Origene Technologies Inc. (Rockville, MD, USA) and subcloned into pcDNA3.1 vector with a C-terminal Flag tag by using the restriction enzymes *Kpn*I and *Xho*I. NLRX1 N-ter (amino acids 1–156), Δ N-ter (amino acids 156–975)

and LRR (amino acids 564–975) were generated by PCR using standard procedures and were fully sequenced.

Bacterial infections. HEK293 and HeLa cells were infected with *Shigella flexneri* strain M90T AfaE (multiplicity of infection = 100; optical density 0.5) as described previously (Girardin et al, 2001).

Expression plasmids, transient transfections and luciferase assays. The empty vector pcDNA3.1, NF-κB- and ISRE-reporter Igκ-luciferase were obtained from Invitrogen. β-gal (pCMV-βgal) was obtained from Clontech (Palo Alto, CA, USA). Expression plasmids encoding p53, HIF-1α, p53-luciferase and HIF-1α-luciferase were a gift from M. Ohh (University of Toronto); human MyD88 and IPS-1 expression vectors were from J. Tschopp (UNIL, Lausanne, Switzerland); AP-1-reporter luciferase was from K. Fitzgerald (University Massachusetts).

Transfections and luciferase assays were carried out as described previously (Girardin et al, 2003).

Immunofluorescence and confocal microscopy. HeLa cells transfected for 18 h with Flag-tagged NLRX1 or NLRX1 deletion constructs were fixed with PFA 4%/Triton X-100 0.01% in PBS, and then saturated in 1% PBS–BSA (bovine serum albumin; Sigma). Cells were incubated with primary and secondary antibodies in 5% PBS–BSA for 2 × 30 min and rinsed in PBS. When required, samples were then incubated with DAPI (5 min) or actin–phalloidin (20 min). For classical immunofluorescence, images were obtained using a Carl Zeiss Axiovert 200 microscope imaging system. Confocal microscopy analyses were carried out using an upright Zeiss LSM510.

Subcellular fractionation and western blotting. Subcellular fractionation of NLRX1-Flag transfected HEK293 cells was carried out as described previously (Desagher et al, 1999). Cell lysis for protein analyses and immunoblotting were carried out according to standard procedures as described previously (Girardin & Yaniv, 2001).

Measurement of ROS production. HeLa cells were transfected for 18 h with Flag-tagged NLRX1 expression constructs or PCDNA3.1. Intracellular ROS generation was measured by using the fluorescent probe 5-(and-6)-chloromethyl-2′,7′-dichlorodihydro-fluorescein diacetate, acetyl ester (CM-H$_2$DCFDA; Molecular Probes Inc., Eugene, OR, USA). After different stimuli, cells were trypsinized and pooled with spontaneously detached cells present in cell culture supernatants. After rinsing, cells were resuspended in PBS–BSA and incubated for 15 min at 37 °C with 10 mM CM-H$_2$DCFDA. Radical formation was assessed by flow cytometry in a FACSCalibur flow cytometer (Becton Dickinson, San Jose, CA, USA). Ten thousand events were evaluated for every analysis.

Activation of caspases. Activation of caspase 3 and caspase 8 was determined by immunofluorescence by using antibodies specific for the cleaved form of the caspases, following the manufacturer's recommendations (Cell Signaling). HeLa cells overexpressing NLRX1 or not were treated with staurosporine (2 μM) or TNF (10 ng/ml) with CHX (0.5 μg/ml) for 2 h.

Expression profile of NLRX1. NLRX1 expression in a panel of 24 human tissues was determined by using the Human Rapid-Scan expression Panels (Origene Technologies Inc.). The levels of NLRX1 among the 24 tissues are expressed as relative units normalized for human β-actin expression. Semiquantitative reverse-transcriptase PCR was carried out for NLRX1 and β-actin on RNA samples purified on columns (Qiagen, Mississauga, ON, Canada) from HeLa, HEK293T, MCF-7, THP-1, Jurkat and Ramos cells.

Supplementary information is available at *EMBO reports* online (http://www.emboreports.org).

CONFLICT OF INTEREST
The authors declare that they have no conflict of interest.

REFERENCES
Akira S, Takeda K (2004) Toll-like receptor signalling. *Nat Rev Immunol* **4:** 499–511
Desagher S, Osen-Sand A, Nichols A, Eskes R, Montessuit S, Lauper S, Maundrell K, Antonsson B, Martinou JC (1999) Bid-induced conformational change of Bax is responsible for mitochondrial cytochrome c release during apoptosis. *J Cell Biol* **144:** 891–901
Fritz JH, Ferrero RL, Philpott DJ, Girardin SE (2006) Nod-like proteins in immunity, inflammation and disease. *Nat Immunol* **7:** 1250–1257
Girardin SE, Yaniv M (2001) A direct interaction between JNK1 and CrkII is critical for Rac1-induced JNK activation. *EMBO J* **20:** 3437–3446
Girardin SE *et al* (2001) CARD4/Nod1 mediates NF-κB and JNK activation by invasive *Shigella flexneri*. *EMBO Rep* **2:** 736–742
Girardin SE *et al* (2003) Nod1 detects a unique muropeptide from Gram-negative bacterial peptidoglycan. *Science* **300:** 1584–1587
Gloire G, Legrand-Poels S, Piette J (2006) NF-κB activation by reactive oxygen species: fifteen years later. *Biochem Pharmacol* **72:** 1493–1505
Golstein P, Kroemer G (2007) Cell death by necrosis: towards a molecular definition. *Trends Biochem Sci* **32:** 37–43
Meylan E, Tschopp J, Karin M (2006) Intracellular pattern recognition receptors in the host response. *Nature* **442:** 39–44
Ohtsuka T, Ryu H, Minamishima YA, Macip S, Sagara J, Nakayama KI, Aaronson SA, Lee SW (2004) ASC is a Bax adaptor and regulates the p53-Bax mitochondrial apoptosis pathway. *Nat Cell Biol* **6:** 121–128
Seth RB, Sun L, Ea CK, Chen ZJ (2005) Identification and characterization of MAVS, a mitochondrial antiviral signaling protein that activates NF-κB and IRF3. *Cell* **122:** 669–682